STUCK IN A MOMENT: A VIEW FROM THE MIRE

Patrick Egan, Jack Stone, Jacob Ricker, and Jay Hendricks
National Institute of Standards and Technology
100 Bureau Drive, Gaithersburg, MD 20899

INTRODUCTION

The next-generation pressure standards will be realized via gas density and the equation of state. One way to access the density is through a measurement of gas refractivity, underpinned by the theoretical calculations that predict the relationship between density and refractivity. At present, calculations with sufficient accuracy that link refractivity to density are only available for helium. To measure helium refractivity we employ interferometry to make ultraprecise measurements of the optical length of gas-filled cells and cavities. The refractivity of helium at atmospheric pressure is about 3.2×10^{-5}: to measure this to 10^{-6} fractional uncertainty—our goal for a pascal realization—would require the measurement of a 15 cm optical length with 4.5 pm accuracy.

We are pursuing two approaches to the measurement of refractivity: a Fabry–Perot (FP) cavity-based system with four interferometers, which we call a variable-length optical cavity (VLOC), and a cell-based heterodyne interferometer, which we call a monolithic interferometer for refractometry (MIRE). Both these optics have been built to precise geometric constraints by silicate-bonding.

The VLOC will measure refractivity as the difference between two 15 cm displacements, one in vacuum and one in helium (where gas pressure and temperature are kept constant during the motion). In actuality we have three interferometers in vacuum surrounding a central interferometer in helium. The main challenge was to minimize the Abbe error: the Abbe offset in this measurement is the deviation of the central interferometer mode from the geometric center of the outer three interferometer modes. In order to minimize the Abbe error, the VLOC has been built with an Abbe offset of less than 70 µm. This feat means that keeping the Abbe error below 1 pm will require measurement and control of angle to better than 20 nrad, which is relatively straightforward given the picometer resolution of FP interferometry. Another feature of the VLOC is that it relies on the flatness of an optical flat to ensure parallel beams in multiple optical cavities and minimize errors associated with beam walk across imperfect optical surfaces. This requires that local surface slopes have a variation ideally held to less than 1 µrad, where the slopes of interest are on a spatial scale of the cavity mode size (sub-millimeter). Many high-precision optics—including optics with better than $\lambda/100$ figure—may not achieve this specification.

In the case of the MIRE, refractivity will be measured as the change in pathlength through a gas cell, as the cell is filled from vacuum to some pressure. One benefit of a 25 cm multipass gas-cell compared to a 15 cm FP cavity is that it has less stringent requirements on the accuracy and stability of the length metrology, and the fact that the experiment can be performed without motion is a great simplification; on the other hand, a heterodyne interferometer has much lower resolution, and cell window thinning caused by changing pressure can contribute a systematic error of several hundred parts per million. To cancel this systematic error we plan to make refractivity measurements through cells of different lengths but with almost identical material properties, borehole and window geometries, and beam incidence. This last requirement—beam incidence—has motivated us build an interferometer that has four beams parallel to two planes within ±85 µrad.

This proceeding describes the features of both optics,—VLOC and MIRE—the geometric requirements that had to be met to achieve our desired measurement precision, and the steps we have taken to build the optics and satisfy these geometric requirements.

VLOC

A general overview assembly of the VLOC is shown in Fig. 1, and the principle behind the measurement is described in more detail in Ref. [1]. At the heart of the device are four Fabry–Perot (FP) cavities, formed on two optics, a parallel mirror plate and a concave mirror assembly. A photograph of the optics is shown in the inset of Fig. 1: three outer FP cavities in vacuum surround an inner FP cavity which is to be sealed in a bellows and filled with helium (the bellows is not shown

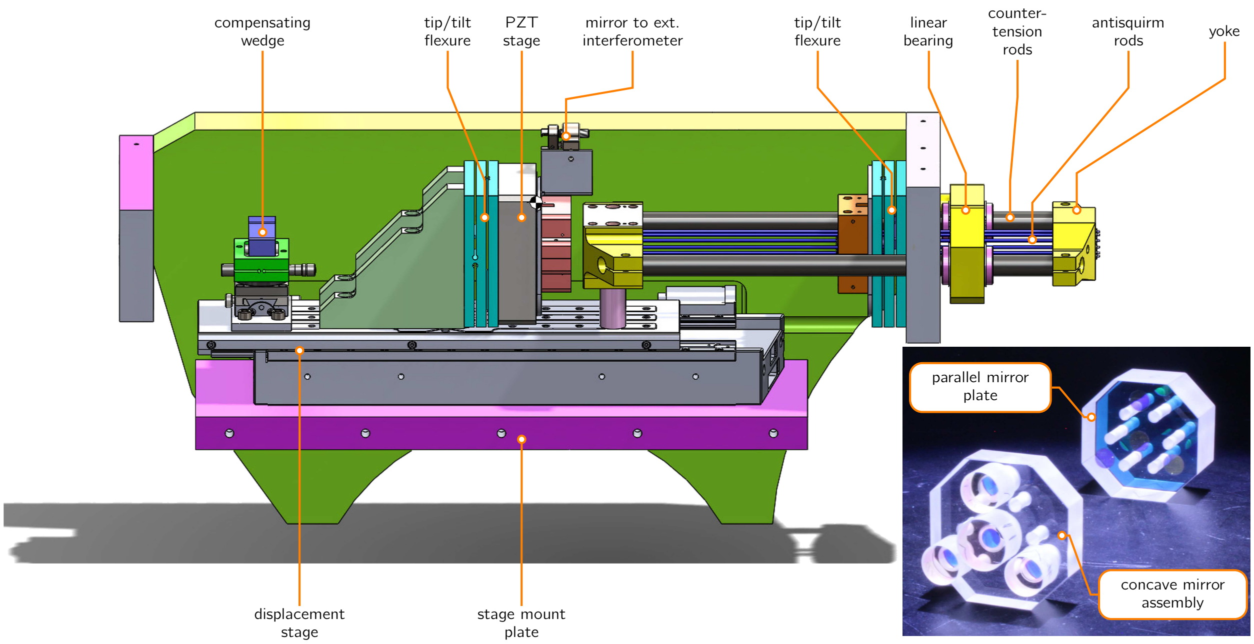

FIGURE 1. The VLOC apparatus consists of a fixed parallel mirror plate inside the tip/tilt flexure at right, and a moving concave mirror assembly inside the PZT stage at left. The displacement stage gives 15 cm of travel, while the PZT stage makes fine adjustments to maintain angular alignment below 20 nrad at the opposite ends of the travel. The inset photograph shows the interferometer optics: concave mirror assembly and parallel mirror plate. The concave mirror assembly has four mirrors silicate-bonded to precise geometric constraint. The span of the octagons are 38 mm.

in Fig. 1). The octagonal shape of the VLOC optics owes its origin to alternative design scenarios that envisioned the bellows sealed to the glass with an o-ring and clamped at four corners; the design we are currently pursuing has the bellows transitioned to glass, and the glass monolithically bonded to the octagon. The six 3.2 mm diameter holes around the center of the octagons are for (tensioned) bellows antisquirm rods: in the mechanicals of Fig. 1, these holes are redundant on the concave mirror assembly.

The concave mirror assembly is housed in the PZT stage which sits on a linear translation stage. In the typical mode of operation the inner cavity will be filled to about 10^5 Pa of helium, and its length is to be changed from 15 cm to 30 cm by the translation stage. (The pressure of helium inside the bellows will be generated by a piston gage: the pressure will be unknown, but constant to $10^{-6} \cdot p$ independent of the volume change.) The outer cavities in vacuum will measure the displacement ΔL, and also monitor pitch/yaw errors in the motion: the PZT stage will be adjusted to correct these motion errors to below 10 nrad. The inner cavity in helium will measure a change in optical length of $n\Delta L$, and thus the difference between the displacements in the outer and inner cavities is a measure of refractivity $n - 1$. This measure of helium refractivity at a known temperature can be used to realize the pascal, as discussed for example in Refs. [2, 3]. In other words, we will use the measured helium refractivity to determine the unknown pressure generated by the piston gage.

These refractivity measurements are expected to happen in the near future. In addition to pitch/yaw at sub-10 nrad, we will also be monitoring straightness/flatness at sub-1 µm: the metrology supporting this apparatus is a large undertaking and will not be described here. The purpose of this section is to describe the characteristics of the interferometer optics at the heart of the VLOC.

Parallel mirror plate

The parallel mirror plate consists of four mirrored portions, (6.5 ± 0.5) mm in diameter, coated on a 20 mm thick, flat substrate. The HR coating was specified as 99.7 % at 633 nm and 1542 nm. (The mirrored portions were masked so that the bellows to glass transition can be bonded and sealed to bare glass on the parallel mirror plate.) Since the mirrors are deposited directly on the plate, the plate had to be wedged at 9 mrad to avoid parasitic reflections entering the cavities (an extra precaution in addition to the AR coating on the back-surface). Because we intend to translate the concave mirror assembly by ΔL = 15 cm, motion errors during translation will inevitably cause beam walk across the parallel mirror plate, and if the mirrored portions are out-of-parallel by ϕ, this beam walk effectively introduces an alignment error between the interferometers approximately $n\Delta L(\frac{\phi^2}{2} + \theta\phi)$ [1]. Here, θ is the misalignment of the central mode direction with the direction of the displacement of the moving mirrors, and $\theta + \phi$ is the misalignment of one of the outer inteferometers. Typically, θ is much larger than ϕ. It will vary with position due to the stage straightness (about 2 µm) and due to roll (30 µrad), so that it is typically larger than 7 µrad regardless of how well overall alignment is achieved. The modes of the three outer interferometers are on a "bolt circle" of 13 mm radius, and the mode diameter is about 0.3 mm: the specification requested of the manufacturer was that all four mirrored regions were to be parallel to 1 µrad, and that surface spatial variations were to be less than 1 nm/mm. It is notable that a $\lambda/100$ surface flatness would not necessarily satisfy this unique parallelism requirement. The manufacturer achieved the 1 µrad parallelism before coating, but stresses induced by the masked coatings changed surface form. The parallel mirror plate was subsequently measured at NIST with a Fizeau interferometer. In Fig. 2 we show surface flatness for each of the outer mirrors relative to the central mirror. The slope of the coatings are within 2 µrad of parallel (ie, ϕ = 2 µrad) to one another, which means that misalignment errors between central and outer interferometers should contribute less than 2 pm error to the displacement measurement. (Interestingly and not apparent in Fig. 2, is that the slope of the coatings relative to the substrate is 15 µrad, and the height of the mirror stacks are about 6.5 µm.)

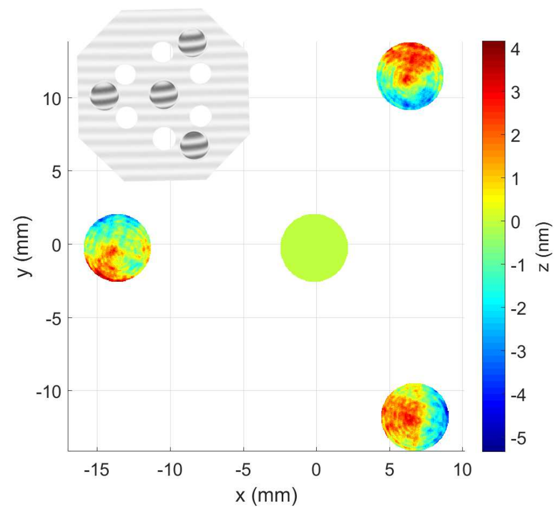

FIGURE 2. Profile of the four HR-coated regions of the parallel mirror plate: The slopes of the three outer coated areas relative to the central coated area are within 2 µrad. Inset: fringes on the Fizeau flatness interferometer.

Concave mirror assembly

The concave mirror assembly is a complicated optic. Its main requirement was to maintain a very stable relationship between the inner and outer mirrors, and also to keep the Abbe offset below 100 µm. For the symmetric case, this is equivalent to saying that the centers of curvature of the three outer mirrors must be located on a circle whose center is concentric within 100 µm of the center of curvature of the central mirror. To our knowledge it is not presently feasible to polish multiple concavities into one substrate and meet this 100 µm concentricity requirement, so positioning and bonding four separate mirrors to one baseplate seemed the viable solution. Additionally, the central interferometer (and the bond between the optics and the bellows-to-glass stub) needs to be leak-tight, and any bonding technique must be ultrastable. These requirements led us to conclude that silicate-bonding [4] was the best (if not only) solution.

The optic consists of a 10 mm thick baseplate (parallel window) with four 6 mm holes drilled through it to allow beam transmission. The four concave mirrors were face-bonded to the parallel window using silicate-bonding, following the LIGO recipe [5]: we used a 4 : 1 ratio of distilled water to sodium-silicate solution, approximately 0.8 µL/cm^2 solution per bond area, and all surfaces were flat to $\lambda/10$. Our approach of face-bonding four separate concave mirrors to a flat baseplate means that a flat annulus must remain on the substrate into which the concavity is polished. It is also desirable that the annulus of the central mirror be as large as possible to minimize leak rates. These requirements must be put in context to a size constraint of 38 mm-square which was placed on our baseplate by the aperture of the PZT stage: all this meant that our inner mirror substrate had a diameter of 13.5 mm and

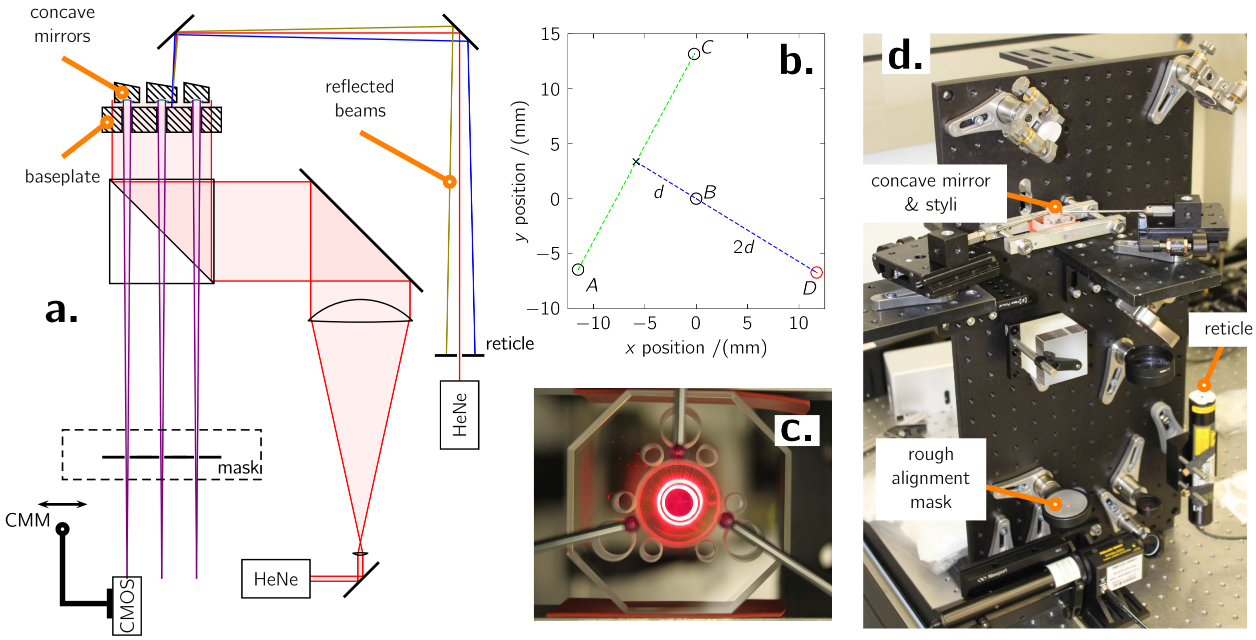

FIGURE 3. (a) Schematic of the jig used for positioning and bonding the concave mirror assembly. (b) The position of the third outer mirror D was found as a projection of the distance 2d through the center B from the midpoint of the line AC: the points A, B, C, D refer to the locations of the mirror focal points. (c) Photograph of center mirror located by ruby styli while bonding. For scale, the diameter of the center mirror is 13.5 mm. (d) The actual jig being used for bonding with the rough alignment mask. To bond the final mirror, the mask was removed, and a camera attached to the ram of a CMM probed the mirror focal points.

the outer mirrors had diameters of 10.5 mm; we specified a diameter on the extent of the concave polish of (7 ± 1) mm. The sagitta of a 0.5 m arc extending 7 mm is only 3 µm, and not only was our tolerance on polish depth/diameter challenging, the best that could be done with centering the polish relative to the mirror substrates was ± 1 mm. The lack of concentricity in the concave mirrors meant that we could not use the mirror substrate as a dimensional reference: we had to position and bond the mirrors while looking at their actual focal points. Also note: The lack of concentricity between the concave polish and the coating mask meant that the focal point was the only point at which we could reliably gage the relative locations of the four interferometer modes. (The coating stack was also undersized relative to the concave polish, so as to permit face bonding between the baseplate and outer annulus of the mirror substrate.)

The principle behind assembling the optic was to nudge the mirrors around so that the locations of their focal points met the near zero-Abbe offset requirement. For nudging the mirrors we used three ruby styli mounted on manual translation stages, shown in Fig. 3(c). In practice and for the most reliable bonding, the assembly proceeded by first bonding the inner mirror and two of the outer mirrors in a cleanroom with rough alignment, and then bonding the last outer mirror in a lab with a coordinate-measuring machine (CMM) that told us precisely where the focal point had to be. Our assembly jig, shown in Figs. 3(a) and (d), worked as follows: We used a $\times 300$ beam expander and HeNe laser to produce a collimated beam of about 100 mm diameter, and this extra large beam was directed to the baseplate. (As mentioned previously, the separation between the outer mirrors is 26 mm, so 50.8 mm optics offered a large enough aperture.) When a concave mirror was placed on the baseplate, its coating reflected a very small part of the large collimated beam and focused it to a point at its focal length. For coarse positioning of the first three mirrors in the cleanroom, we used an aluminum plate as a rough alignment mask, which had 0.2 mm diameter holes drilled in locations where the centers of curvature were nominally supposed to be; we bonded the inner and two outer mirrors so that three beams reflected and focused from these mirrors passed through the holes in the mask.

This rough alignment and bonding was judged by eye, and is shown in process in Fig. 3(d).

For ease and convenience, we did not aim to achieve an equilateral triangle with the focal points of our first three coarsely positioned mirrors, and therefore lacking symmetry, the zero-Abbe position of the third outer mirror does not follow the concentric circle geometry previously mentioned: instead, as in Fig. 3(b), the third outer mirror was positioned a precise distance along a line from the mid-point of the line between the two outer mirrors projected through the point of the central mirror. When positioning the final mirror the coarse alignment mask was removed, and we probed the focal point of beams reflected from the mirrors with a camera mounted to a CMM. [For reference, an analogous setup with a camera on a CMM is shown in Fig. 4(c).] The positional uncertainty of the CMM was 2 µm. We used the centroid of the camera image as the reference, and moved the camera (ram of CMM) so that the centroid of each beam was referenced to the same pixel location: we had reproducibility of 6 µm locating the focal points of the three coarsely positioned mirrors. As mentioned previously, there is a lack of concentricity between the concave polish and coated region, which meant that the relative separations of the reflected beams changed as a function of distance (typically less than 1.7 µm/mm) and we had to translate the camera at the focal plane: we were confident of locating the focal plane to 3 mm. Once the focal points of the three coarsely placed mirrors were found, the position of the third outer mirror was calculated, the camera moved to that calculated point, and the mirror was nudged to position and bonded so that its focal point was at the reference position on the camera. We achieved an Abbe offset of 62 µm.

A minor complication in the concave mirror assembly is that the concave mirrors are polished into wedged substrates to avoid parasitic cavities. Since the concave mirror assembly is the moving part of the VLOC, beam alignment and coupling into the cavities would be translation dependent. To mitigate this problem, we employ the compensating plate shown in Fig. 1, which has a wedge nearly identical to that of the concave mirror substrates but rotated in azimuth so that the two prisms effectively cancel. However, effective cancellation of the beam deviation demanded that we also ensure the rotation of each mirror—wedge orientation—was nominally the same. To achieve this, we used a second laser as a beam pointer, also shown in Fig. 3(a) and (d). For the bonding of each mirror, we directed the beam pointer so that it passed through the outer edge of the mirror substrate. This resulted in two reflections: one from the wedged back-surface of the mirror and one from the baseplate. (In actuality, the reflection from the baseplate overlapped the reflection from the front-surface of the mirror substrate—and this became a single reflection after bonding.) We positioned a reticle in front of the pointing laser: the reticle was simply a line on a piece of paper placed on the laser head (ie, the reflection was deliberately directed almost back into the laser tube). Our premise was that if each mirror was rotated such that the two reflections end up on the line of the reticle, then the wedge of each mirror was orientated the same. Our premise relied on the fact that the baseplate is flat, and that the reticle did not rotate between the bonding of each mirror. However, the approach was independent of the angle and relative location of the incident beam.

MIRE

MIRE is based on the classical Tanaka-style interferometer [6], in which we have a gas cell in the measurement arm and a vacuum cell in the reference arm. We actually implement this in a multipass scheme with a triple-cell, where either the central cell or the two outer cells can serve as a reference arm while the other serves as the measurement arm, as in Fig. 4(a). The body of the triple-cell is a single piece of borosilicate crown glass with three holes through it, and at each end a single piece of glass is silicate-bonded forming windows for the three holes: knowledge of cell length is a prerequisite for accurate refractivity measurements, and the thin and repeatable (100 ± 50) nm bond interface allowed us to accurately measure cell length on a CMM before the windows were bonded. Unlike the VLOC, which is designed in such a manner that it can be operated at constant pressure, the critical measurand for the MIRE is a change in optical pathlength when gas is admitted to the measurement arm. Effects of pressure distortions [7] must be taken into account by building at least two such triple-cells, one short and one long. This is a simpler alternative than a possible approach based on a variable length cell, analogous to the VLOC but with a moving window replacing the moving mirror, as discussed next.

In most refractometers such as the MIRE, the reference and measurement beams pass through the same thickness of glass windows. This arrangement will largely compensate various effects including thermal variations of the windows and changing pathlengths that will occur if the window tilts. The compensation also will eliminate the effect of any uniform wedge in window thickness, which might otherwise cause an unacceptably large variation in pathlength accompanying even microscopic changes in where the beam passes through the window. However, the compensation will be imperfect due to non-flatness of window surfaces, and the situation for a variable length cell with a moving window then becomes entirely analogous to the problem of beam-walk across a non-flat mirror coating in the VLOC, where variations in surface slopes of the optical element between the positions of the measurement and reference beams will give rise to errors. As a practical matter the problem is somewhat more difficult to remedy for a cell-based approach than for the VLOC. For this reason and for reasons of mechanical simplicity, we completely abandon the moving window scheme with its requirement of having equal glass paths independent of cell length. Our approach is based on two (or more) fixed-length cells, where the window thicknesses will ideally be matched at the micrometer level but need not be matched at the picometer level! The critical measurement is not a change in pathlength for a known displacement but changes in pathlength when gas is admitted to the short and long cell. Under these circumstances the requirement that the window optical pathlength is independent of cell length is replaced by a requirement that, for any given fixed length, the variation of the window pathlength with cell pressure is the same for the short and long cells. This can be assured if the window does not move transversely to the beam when pressure is changed (beam-walk), and if window thinning due to the pressure change is the same for both cells. The second requirement is more demanding than the first but can be met if the dimensions and geometry of the windows are near-identical, if the mechanical and optical properties of the windows are near-identical (glass made from the same melt), and if the beams pass through all windows at approximately the same position relative to the underlying holes. This last requirement means that beams must be parallel to each other so that they pass through the same window position in cells of different length. We now describe how the interferometer was built, and the steps we have taken to ensure similar beam incidence between long and short triple-cells.

For the MIRE apparatus stability is a chief concern, and our requirement is rather challenging: a thermodynamic measurement like refractivity has a timescale of several hours (0.1 mHz), and we need the interferometer to be stable below 100 pm during the measurement. By comparison, if extrapolated to 0.1 mHz, the stability requirement of the LISA Pathfinder interferometer is 5 nm [8]. We follow the LISA approach for interferometer stability, and have all optics silicate-bonded [4] to a 42 cm × 15 cm × 2.5 cm fused silica baseplate. A photograph and schematic of the baseplate part of the interferometer are shown in Fig. 4(a) and (b). All bonding surfaces were optically polished to $\lambda/10$ flatness: the baseplate has $\lambda/10$ local flatness over 6.5 cm^2, and 3λ global flatness. Most optics were bonded directly to the baseplate (fiber launch, polarizing-beamsplitters, mirrors, and Jamin-beamsplitter); whereas others were face-bonded to one another (polarizer and waveplates to polarizing-beamsplitters, collimating lenses to the fiber launch, and wedge prism-pairs to a mount block). The face-bonding was done with uncoated surfaces, and we typically observe reflections less than 0.03 % from the bond interface.

Fiber-launching (beam-pointing) began by inserting flat-polished and antireflection (AR) coated fiber ferrules into 20 µm clearance holes which set the 22 mm separation between the beams. The ferrules were epoxied into this tight-fit, and the depth of insertion was adjusted to collimate the beams at 2.1 mm diameter. In process we found a shear plate and viewer the most practical method of judging collimation, and we subsequently used a wavefront sensor to measure beam divergences of 0.190 mrad and 0.254 mrad, which are close to the 0.192 mrad of perfect collimation. Two aspheric lenses (plano-convex) were face-bonded along their 1 mm outer annulus to the fiber launch block, and were nudged into place with three ruby styli on micrometer stages to set the beams to be parallel. (The collimating lenses are AR-coated, and this outer annulus was the one bond that involved a coated surface.) We configured a CMM to translate a camera parallel to the polished baseplate surface, and beam-pointing was adjudged by looking at the image-centroid at near and far positions. See

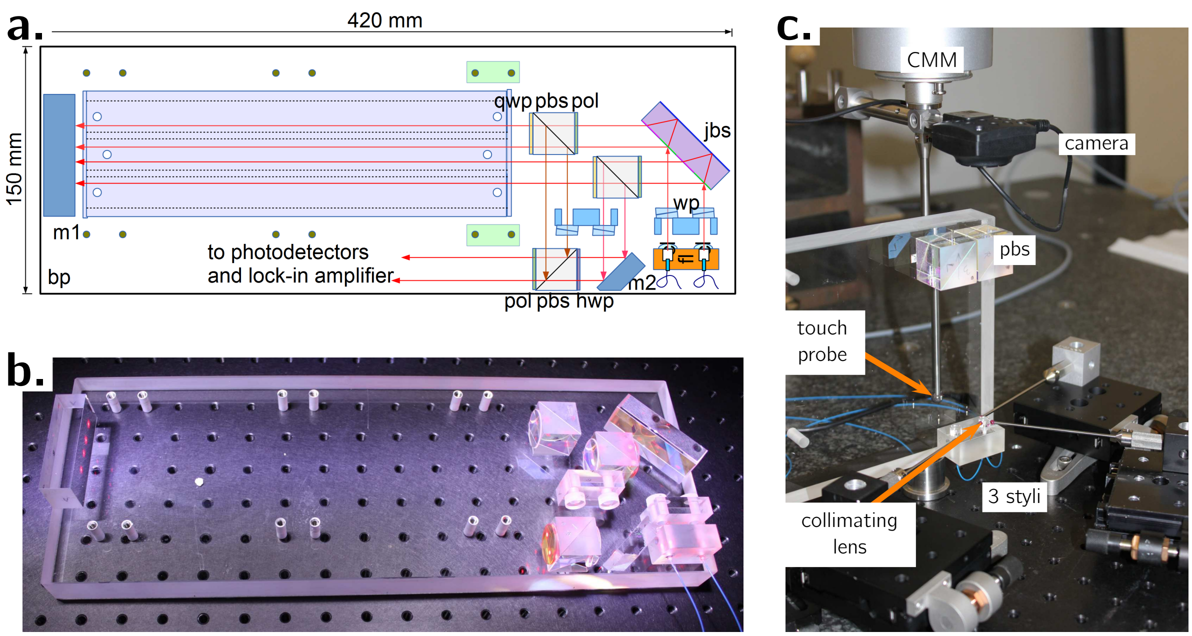

FIGURE 4. (a.) Schematic of the interferometer, with components drawn to scale. (b.) Photograph of MIRE, without gas triple-cell. Threaded invar inserts are epoxied into the baseplate to clamp the inlet/outlet o-ring flanges to the triple-cell. (c.) Setup to align beam-pointing. The collimating lens is positioned by three styli on translation stages. The camera on the CMM is vertically translated by about 20 cm: the camera measures the beam centroid at near and far positions. A touchprobe is used to build a coordinate system so that the camera runs parallel to a desired plane (eg, the plane of the polished baseplate).

Fig. 4(c) for how this setup looked in practice. We achieved beams out-of-parallel to one another by (220 ± 15) µrad. This residual error in beam alignment necessitated the 9 mrad wedge prism-pairs to further correct beam-pointing, a point we will return to momentarily.

After the fiber launch the two beams are separated into four by a Jamin-beamsplitter, which consists of alternating 0.25 % and 50 % reflective-coated portions on its front surface and a 99.5 % reflective-coating on its back surface; the parallelism on the Jamin-beamsplitter was 10 µrad, and its thickness sets the 12 mm reflected beam separation. The four beams reflected from the Jamin-beamsplitter are polarized with a 10^5 extinction ratio, and a quarter-waveplate set the polarization state such that more than 99.3 % of the beam returning from the fold-mirror was reflected by the polarizing-beamsplitter. The polarizing-beamsplitters are epoxy-free, and the transmitted beam deviation through the assemblies was as large as 250 µrad; which is why the aforementioned lens bonding was done with the beamsplitters temporarily in place, as shown in Fig. 4(c). The bonding surface of the fold-mirror and Jamin-beamsplitter were polished within 100 µrad of perpendicular to the coated surfaces. Two 0.4 mm diameter aperture jigs were located relative to the straightedge of the baseplate and temporarily tacked in place at the extremities between the Jamin-beamsplitter and eventual location of the fold-mirror: the Jamin-beamsplitter was nudged into position and bonded so as to maximize the intensity passing through both apertures on a large-area photodetector. At this point of the build, we returned to the CMM and locked-in the final beam-pointing with the wedge prism-pairs. The CMM was configured to run parallel to the polished surface and straightedge of the baseplate: referencing beam alignment to both these planes is advantageous for reproducible positioning of triple-cells of different length. We achieved beam alignment parallel to these two planes within ± 85 µrad. The resolution of our beam-pointing setup was about 50 µrad, as determined by the 6 µm reproducibility of the image centroid, the few micrometers form of the planes to which the CMM was configured to run parallel, and the 15 cm travel of the CMM axis. In hindsight, we believe an improvement factor of two to three could be gained with a more clever arrangement on the CMM (ie, more travel) and with wedge prism-pairs closer to 1 mrad (our choice of 9 mrad was based on what is available off-the-shelf).

The aforementioned aperture jigs were once again tacked in place and referenced to the straightedge, and the fold mirror was nudged into position and bonded so as to maximize the intensity returning through the two apertures (as observed reflected by the polarizing-beamsplitters); this setup ensured that alignment of the returning beams were referenced to the baseplate straightedge within 100 µrad; subsequent positioning of the triple-cells (of different lengths) can initially be achieved by caliper measurements referenced to this straightedge, and reproducibility ensured by hard-stops (ie, spheres epoxied in place). The result of these efforts is that when we measure gas refractivity in triple-cells of different lengths, we are confident beam incidence is the same for all window pairs to within 0.2 mm. After the beams are returned through the triple-cell and reflected from the beamsplitters, they are combined in a final halfwaveplate-beamsplitter-polarizer optic and sent to photodetectors, outside the vacuum chamber in which the MIRE sits. Before interference, we employed another wedge prism-pair to optimize visibility: these prism-pairs are a minor weakness of the design, because the glass pathlength imbalance introduces a temperature dependent drift of about 26 pm/mK; during refractivity measurements we typically have sub-mK temperature stability. Differential phase is measured with a lock-in amplifier. As of writing, MIRE is demonstrating sub-50 pm stability over 15 h  (min: -44 pm, max: 45 pm, 600-s averaging), which in a 12.5 cm long triple-cell would correspond to a fractional error of less than $2\times10^{-6}\cdot p$ for a pascal realization at 200 kPa. We are in the process of taking refractivity data in triple-cells of different lengths, and these measurements will be the subject of a future article.

OUTLOOK

We have described the precision engineering behind optics at the heart of two ultraprecise refractometers built at NIST, the VLOC and MIRE. The refractometers will be used to realize the pascal via measurements of gas density and the equation of state. We described some of the unique features of the VLOC optic, among which is a 2 µrad parallelism between mirrored regions 26 mm apart, a 2 nm/mm local flatness, and an Abbe offset of 62 µm. The critical feature of MIRE is that, while keeping the build quasi-monolithic and ultrastable, two pairs of beams launched from two fibers have been aligned to two planes within $\pm$85 µrad of parallel.

At the present time, MIRE is running and taking data, and the experiment will soon be described in more detail. The VLOC apparatus is nearing completion, and initial characterization tests are expected to begin late 2017.

REFERENCES

[1] Stone J, Egan P, Hendircks J, Strouse G, Olson D, Ricker J, et al. Metrology for Comparison of Displacements at the Picometer Level. In: Precision Engineering and Nanotechnology V. vol. 625 of Key Engineering Materials. Trans Tech Publications; 2014. p. 79–84.

[2] Schmidt JW, Gavioso RM, May EF, Moldover MR. Polarizability of Helium and Gas Metrology. Physical Review Letters. 2007 Jun;98:254504.

[3] Puchalski M, Piszczatowski K, Komasa J, Jeziorski B, Szalewicz K. Theoretical determination of the polarizability dispersion and the refractive index of helium. Physical Review A. 2016 Mar;93:032515.

[4] Gwo DH. Ultra-precision bonding for cryogenic fused-silica optics. In: Heaney JB, Burriesci LG, editors. Cryogenic Optical Systems and Instruments VIII. vol. 3435. SPIE; 1998. p. 136–142.

[5] Armandula H, van Veggel M. Silicate bonding procedure (hydroxide-catalysis bonding). LIGO Scientific Collaboration; 2010. Document #: E050228-v2.

[6] Tanaka M, Yamagami T, Nakayama K. Linear interpolation of periodic error in a heterodyne laser interferometer at subnanometer levels. IEEE Transactions on Instrumentation and Measurement. 1989 Apr;38(2):552–554.

[7] Birch KP, Downs MJ, Ferriss DH. Optical path length changes induced in cell windows and solid etalons by evacuation. Journal of Physics E. 1988;21(7):690–692.

[8] Audley H, Danzmann K, Marín AG, Heinzel G, Monsky A, Nofrarias M, et al. The LISA Pathfinder interferometry: hardware and system testing. Classical and Quantum Gravity. 2011;28(9):094003.